Colloids and Surfaces B: Biointerfaces 92 (2012) 340–347

Contents lists available at SciVerse ScienceDirect

Colloids and Surfaces B: Biointerfaces

journal homepage: www.elsevier.com/locate/colsurfb

Deposition kinetics of MS2 bacteriophages on clay mineral surfaces

Meiping Tong[a,*], Yun Shen[a], Haiyan Yang[a], Hyunjung Kim[b,**]

[a] The Key Laboratory of Water and Sediment Sciences, Ministry of Education, College of Environmental Sciences and Engineering, Peking University, Beijing 100871, PR China
[b] Department of Mineral Resources and Energy Engineering, Chonbuk National University, Jeonju, Jeonbuk 561-756, Republic of Korea

ARTICLE INFO

Article history:
Received 31 August 2011
Received in revised form 9 December 2011
Accepted 9 December 2011
Available online 21 December 2011

Keywords:
Bacteriophage MS2
Clay
Deposition kinetics
QCM-D
DLVO

ABSTRACT

The deposition of bacteriophage MS2 on bare and clay-coated silica surfaces was examined in both monovalent (NaCl) and divalent ($CaCl_2$ and $MgCl_2$) solutions under a wide range of environmentally relevant ionic strength and pH conditions by utilizing a quartz crystal microbalance with dissipation (QCM-D). Two types of clay, bentonite and kaolinite, were concerned in this study. To better understand MS2 deposition mechanisms, QCM-D data were complemented by zeta potentials measurements and Derjaguin–Landau–Verwey–Overbeek (DLVO) interaction forces calculation. In both monovalent and divalent solutions, deposition efficiencies of MS2 increased with increasing ionic strength both on bare and clay-coated surfaces, which agreed with the trends of interaction forces between MS2 and solid surface and thus was consistent with DLVO theory. The presence of divalent ions (Ca^{2+} and Mg^{2+}) in solutions greatly increased virus deposition on both silica and clay deposited surfaces. Coating silica surfaces with clay minerals, either kaolinite or bentonite, could significantly increase MS2 deposition.

1. Introduction

The improper discharge of wastewater, the usage of fecal-contaminated water and sludge for agriculture, the artificial groundwater recharge with recycled water, as well as the leakage of septic tanks or pipes have led to the entrance of viruses in the environment [1–5]. Viruses can be transported with water or manure suspensions in natural environment, as a result, pathogenic viruses have been found in well waters and groundwater [6,7]. Pathogenic viruses entering groundwater could pose a great threat to public health [8]. Majority of the outbreaks of waterborne diseases have been associated with groundwater contamination by pathogenic viruses [9–11]. Therefore, understanding the mechanisms that control the transport behavior of virus in the subsurface is of great interest.

Many processes controlling virus transport in natural environment include advection, dispersion, deposition onto and detachment from solid surfaces, and inactivation, among which deposition and inactivation have been regarded as the two most important processes [12–14]. In past decades, great efforts have been directed toward investigating the factors affecting the deposition behavior of viruses onto solid surfaces. Factors such as solution ionic strength [15–18], ion types [19,20], pH [13,18,21,22], flow velocity [23,24], dissolved organic matter [21,25–28], and mineral colloids present in solutions [23,29] have been shown to have great influence on virus deposition. For example, Gutierrez et al. [20] examined the effects of ion types on rotavirus deposition onto silica and found the deposition of rotavirus with the presence of Ca^{2+} in solutions was greater than that with Mg^{2+} in solutions. Walshe et al. [23] investigated the effects of pH, ionic strength, and dissolved organic matter on the transport of MS2 phage in gravel aquifer media. This study showed that decreasing solution pH or increasing solution ionic strength increased virus deposition onto aquifer media, whereas increasing flow rate and the concentration of dissolved organic matter decreased virus deposition. Very recently, Sadeghi et al. [18] also reported the deposition of phage PRD1 on quartz sand increased with decreasing pH and increasing ionic strength.

A number of previous studies have also investigated the effects of properties of solid surfaces on the transport (deposition) behavior of viruses and found the solid (soil) properties such as texture, organic matter contents, metal/metal oxides contents greatly affected virus deposition [16,22,24,29–33]. For example, Chu et al. [31] found the presence of metal oxide in soils could largely enhance virus deposition. Yuan et al. [32] compared the deposition of MS2 on bare silica surfaces versus that on NOM-coated surfaces and showed the presence of NOM on silica surfaces decreased virus deposition. Very recently, by comparing the deposition of viruses onto three types of solid surfaces (aluminum oxide-coated sand, goethite-coated sand, and oxide-removed sand), Attinti et al. [33]

* Corresponding author. Tel.: +86 10 62756491; fax: +86 10 62756526.
** Corresponding author. Tel.: +82 63 2702370; fax: +82 63 2702366.
E-mail addresses: tongmeiping@iee.pku.edu.cn (M. Tong), kshjkim@jbnu.ac.kr (H. Kim).

0927-7765/$ – see front matter © 2011 Elsevier B.V. All rights reserved.
doi:10.1016/j.colsurfb.2011.12.017

reported the deposition of viruses onto aluminum oxide-coated was greatest, followed by goethite-coated sand, and was lowest on oxide-removed sand.

Due to their large cation exchange capacity (CEC) or anion exchange capacity (AEC), clay minerals (ubiquitous present in natural environment) have been widely utilized to remove heavy metals and organic contaminants from wastewater. The adsorption of viruses onto minerals has also been investigated. For example, Lipson and Stotzky [8] investigated the adsorption of Reovirus to clay minerals and found that the deposition of viruses onto clay minerals was significant. Moreover, virus deposition onto montmorillonite was greater than that onto kaolinite. More recently, Syngouna and Chrysikopoulos [34] examined the effects of temperature and agitation on virus adsorption onto clays. These authors found the adsorption of viruses was higher with agitation and increased with temperature. It should be noted that batch experiments in steady states were employed to determine the adsorption (deposition) of viruses onto clay mineral surfaces in previous studies. The deposition kinetics of viruses onto clay surfaces in a continuous flow mode as a function of solution chemistry have not been clearly explored in previous studies. Moreover, direct comparison of deposition of viruses onto two ubiquitous solid surfaces in natural environment, silica and clay surfaces, has never been explored.

To better understand the deposition kinetics of viruses onto clay mineral surfaces, the deposition of bacteriophage MS2 onto clay (bentonite and kaolinite)-coated silica surfaces was determined over a wide range of environmentally relevant ionic strengths and pH in both monovalent and divalent solutions employing a quartz crystal microbalance with dissipation (QCM-D). Our study showed that the deposition of virus onto clay minerals could be significantly influenced by solution ionic strength, ion types, and pH. Under all examined conditions, virus deposition onto clay mineral surfaces was greater than that onto silica surfaces.

2. Materials and methods

2.1. MS2 preparation and characterization

Bacteriophage MS2 was replicated and purified following the methods provided in Yuan et al. [32]. Briefly, MS2 phages were propagated with host bacterial *Escherichia coli* strain 15597 (American Type Culture Center). Following replication, MS2 was purified by centrifugation (8000 rpm for 15 min at 4 °C) (Eppendorf 5804R, Germany) and filtered through 0.22 μm cellulose acetate filters. To settle down the MS2, Polyethylene glycol 8000 (Sigma–Aldrich, St. Louis, MO) and NaCl were introduced into the MS2 supernatant to a final concentration of 10% and 0.6%, respectively. The suspension was then stored in the dark at 4 °C for 10 h. After that, MS2 was collected by centrifugation at 8000 rpm for 20 min at 4 °C. The MS2 pellets were then re-suspended in Milli-Q water. The centrifugation-re-suspension process was repeated one more time. Further MS2 purification was conducted by filtering through 0.22 μm cellulose acetate filters and Amicon Ultra-15 centrifugal filter unit. The stock MS2 solution was then stored in dark at 4 °C until being used for deposition experiments or characterization. The stock solution was freshly prepared every week. MS2 enumeration was performed following the double agar layer procedure plaques forming unit (PFU). The detailed MS2 enumeration protocol can be found in Yuan et al. [32]. It should be noted that only the plates that had from 20 to 300 plaques were used for calculation of MS2 concentration. The stock concentration was found to be $\sim 10^{10}$ PFU/mL. Zeta potentials and sizes of MS2 in examined salt solutions were determined by using a Zetasizer Nano ZS90 (Malvern Instruments, UK) at MS2 concentration of 2×10^8 PFU/mL. The zeta potentials measurements at each condition were repeated 9–12 times and the sizes measurements were repeated 3 times.

2.2. Clay solutions preparation

Bentonite (Sigma–Aldrich, St. Louis, MO) and kaolinite (Fluka, Milwaukee, WI) were used as model clays in this investigation. The molecular weights of bentonite and kaolinite employed in our study are 180.1 and 258.16 g mol^{-1}, respectively. The main chemical components of the bentonite were: SiO_2 ~48.35%, Al_2O_3 ~12.15%, Fe_2O_3 ~8.26%, CaO ~6.68%, MgO ~5.47%, Na_2O ~3.65%, and K_2O ~2.39%, whereas the main chemical components of the kaolinite were SiO_2 ~47.3%, Al_2O_3 ~37.6%, Fe_2O_3 ~0.5%, TiO_2 ~0.4%, Na_2O ~0.1%, and K_2O ~1.8% [34,35]. The BET surface areas of bentonite and kaolinite were 39.3 and 9 m^2 g^{-1}, respectively [34,35]. The clay stock solutions were prepared by dissolving clay powders in Milli-Q water. The particle size of bentonite and kaolinite in Milli-Q water was found to be 554 nm and 712 nm, respectively. Zeta potentials of clay particles (10 ppm) in examined salt solutions were also measured by Zetasizer Nano ZS90.

2.3. Quartz crystal microbalance with dissipation (QCM-D)

A QCM-D E1 system (Q-Sense AB, Gothenburg, Sweden) was utilized to examine the deposition kinetics of MS2 on bare and clay-coated silica surface. QCM-D experiments were performed with 5 MHz AT-cut quartz sensor crystals with silica-coated surface (Batch 081110-3). Before each measurement, the crystals were soaked for 30 min in a 2% SDS solution, rinsed thoroughly with Milli-Q water, dried with ultrahigh-purity N_2 gas, and then oxidized for 30 min in a UV/O_3 chamber (Bioforce Nanosciences, Inc., Ames, IA). The MS2 deposition experiments were performed in a flow-through mode using a peristaltic pump (ISMATEC, Switzerland) operating in clockwise mode. Specifically, the pump was connected to the sensor crystal outlet. The studied solutions, stored in a sterilized 10 mL polypropylene conical tube (Becton Dickinson, Franklin Lakes, NJ) connected to the sensor crystal inlet, were fed through the crystal sensor chamber at a flow rate of 0.1 mL min^{-1}.

2.4. MS2 deposition experiment

The influence of two clay types (adsorbed on silica surfaces), bentonite and kaolinite, on the deposition kinetics of MS2 was examined in this study. To investigate the significance of adsorbed clay on the deposition kinetics of MS2, deposition behavior of MS2 on bare silica surfaces, poly-L-lysine (PLL) hydrobromide coated surfaces (PLL, molecular weight of 70,000–150,000, P-1274, Sigma–Aldrich, St. Louis, MO), and clay-coated surfaces was examined over a wide range of environmentally relevant ionic strength in NaCl (with five ionic strengths ranging from 5 to 100 mM), $CaCl_2$ (with four ionic strengths ranging from 0.5 to 5 mM), and $MgCl_2$ (with four ionic strengths ranging from 0.5 to 5 mM) solutions. MS2 deposition experiments were performed at two pH conditions, pH 6.0 (adjusted with 0.1 M HCl) and pH 9.0 (adjusted with 0.1 M NaOH). This wide range of solution chemistries examined in this study can be commonly found in groundwater [36]. The influent concentration of MS2 suspension for deposition experiments was kept as 2×10^8 PFU/mL.

For the experiments performed on bare silica surfaces, the QCM-D system was pre-equilibrated with desired salt solution (desired ionic strength and pH) for a minimum of 30 min to establish a stable baseline (the shift of average normalized frequency was less than 0.2 Hz within 30 min). After pre-equilibration, MS2 suspension at desired ionic strength and pH (adjusted with 0.1 M HCl or NaOH) was injected into the crystal chamber. The duration of injection lasted for at least 30 min.

For the experiments conducted on favorable (non-repulsive) condition, a layer of positively charged PLL was deposited on silica surfaces prior to the deposition experiments. We followed the method that employed in previous works to adsorb a layer of PLL onto the silica surface [37,38], which was also provided in Supplementary information. Corresponding deposition experiments on PLL-coated silica surfaces were performed over the same ionic strength range with the same MS2 influent concentration as that conducted on bare silica surfaces. A detail about MS2 deposition experiment on PLL-coated surfaces was also provided in Supplementary information.

For deposition experiments conducted on clay (bentonite or kaolinite) coated silica surfaces, the bare silica surfaces were first modified with a layer of positively charged PLL, and then a negatively charged clay (bentonite or kaolinite) solution at 10 mg L^{-1} TOC prepared in 0.1 mM NaCl solution was introduced into crystal chamber. Details of adsorbing clay layer on PLL-coated surfaces can be found in Supplementary information. After coating clay on the surfaces, the salt solution of interest was flowed through the clay-coated surface until a constant baseline was established. The desired MS2 sample (2×10^8 PFU/mL) with the same solution ionic strength and pH was then injected into the flow chamber.

2.5. QCM-D data analysis

For all experiments, the deposition rate of MS2 can be determined from the slope of the initial (linear) portion of the change in normalized frequency Δf_3 versus time curve:

$$k_f = \frac{d\Delta f_3}{dt} \tag{1}$$

The deposition rate at different solution conditions is then presented in terms of the deposition efficiency (α), which is the ratio of the deposition rate on bare or clay-coated silica surfaces (k_{fp}) relative to the corresponding deposition rate obtained on PLL-coated silica surface (k_{fa}):

$$\alpha = \frac{k_{fp}}{k_{fa}} \tag{2}$$

2.6. DLVO energy profiles

DLVO theory was used to calculate the total interaction force between MS2 and substrate surface as a function of separation distance. van der Waals and electrical double layer forces were considered in DLVO theory. The particle–collector interaction force was calculated by treating the particle–collector system as a sphere-plate interaction. The retarded van der Waals forces for sphere-plate configuration can be calculated according to the following equation [39]:

$$f_{vdw} = \frac{A_{132} a_p \lambda(\lambda + 22.232h)}{6h^2(\lambda + 11.116h)^2} \tag{3}$$

where a_p refers to the size of MS2, which was taken from values measured by Zetasizer Nano ZS90 (Malvern Instruments, UK); h is the separation distance between MS2 and plate surface; λ is the characteristic wavelength of interaction, usually taken as 100 nm; A_{132} is the combined Hamaker constant for the particle–water–surface system. The Hamaker constants of 4×10^{-21} J [32,40] and 7.5×10^{-21} J [34] were employed for MS2–water–silica surfaces and MS2–water–clay systems, respectively. Whereas, for the MS2–water–PLL surfaces, the Hamaker constant of 9.0×10^{-21} J was utilized (the detailed calculation process to obtain Hamaker constant of MS2–water–PLL system was provided in Supplementary information).

The electrostatic double layer forces for sphere-plate configurations can be determined according to the following equations [39]:

$$F_{EDL} = 4\pi\varepsilon_e\varepsilon_r\kappa a_p\zeta_p\zeta_c \left[\frac{\exp(-\kappa h)}{1+\exp(-\kappa h)} - \frac{(\zeta_p - \zeta_c)^2}{2\zeta_p\zeta_c}\frac{\exp(-2\kappa h)}{1-\exp(-\kappa h)}\right] \tag{4}$$

$$\kappa = \sqrt{\frac{e^2 \sum n_{j0} z_j^2}{\varepsilon_0 \varepsilon_r kT}} \tag{5}$$

where ε_0 is the permittivity of vacuum; ε_r is the dielectric constant or relative permittivity of water; ζ_p and ζ_c are the zeta potential of the MS2 and the plate surface, respectively; z_j is the ion valence, e is the electron charge; n_{j0} is the number concentration of ions in the bulk solution.

3. Results and discussion

3.1. Characterization of MS2

The sizes of MS2 as a function of solution ionic strength in NaCl, $CaCl_2$, and $MgCl_2$ solutions at pH 6.0 and pH 9.0 were measured in this study. The particle sizes were around 25–35 nm under all examined conditions, indicating that the MS2 suspensions for the deposition experiments were monodisperse. The measured MS2 sizes were consistent with 30 nm reported by Yuan et al. [32].

The zeta potentials of MS2 as a function of solution ionic strength in NaCl, $CaCl_2$, and $MgCl_2$ solutions at pH 6.0 and pH 9.0 were determined and presented in Fig. 1. Under all examined ionic strength conditions in NaCl, $CaCl_2$, and $MgCl_2$ solutions, zeta potentials of MS2 were negative and became less negative with increasing ionic strength at both pH conditions due to the compression of electrostatic double layer at high ionic strengths. The zeta potentials obtained in our study were consistent with those provided by Syngouna and Chrysikopoulos [34]. Under the same ionic strength (i.e. 5 mM), the zeta potentials in divalent salt ($CaCl_2$ and $MgCl_2$) solutions (Fig. 1b and c) were less negative relative to those in monovalent NaCl solutions (Fig. 1a). For example, the zeta potentials of MS2 in NaCl solutions at pH 6.0 are −31.25 mV, whereas the corresponding zeta potentials in $CaCl_2$ and $MgCl_2$ solutions are −9.17 mV and −9.83 mV, respectively. This observation was true for both pH conditions. The less negative zeta potentials observed for MS2 in divalent salt solutions have also been previously reported for other virus e.g. Rotavirus [20]. The complexation of divalent cations with negatively charged functional groups (e.g. carboxyl groups) on MS2 surfaces led to the neutralization of surface charge [41], as a result, the zeta potentials observed in $CaCl_2$ and $MgCl_2$ solutions were less negative. Comparison of the zeta potentials obtained in two divalent salt solutions showed the zeta potentials acquired in $CaCl_2$ solutions were slightly less negative relative to those in $MgCl_2$ solutions due to the greater binding ability of Ca^{2+} with functional groups (e.g. carboxyl groups) on cell surfaces [42]. At the same ionic strength, the zeta potentials of MS2 acquired at pH 6.0 (open symbol) were less negative relative to those at pH 9.0 (solid symbol). This holds true over the whole ionic strength range examined in all salt (NaCl, $CaCl_2$ and $MgCl_2$) solutions. At low pH conditions, the functional groups on MS2 surfaces might be protonated, leading to the less negative zeta potentials at low pH.

3.2. MS2 deposition on PLL-coated silica surfaces

MS2 deposition on PLL-modified silica surfaces was examined in a wide range of solution ionic strengths in NaCl (5–100 mM), $CaCl_2$ (0.5–5 mM), and $MgCl_2$ (0.5–5 mM) solutions at pH 6.0 and pH 9.0. Deposition rates decreased slightly with increasing ionic strengths in monovalent NaCl solutions at both pH 6.0 (open symbol) and 9.0

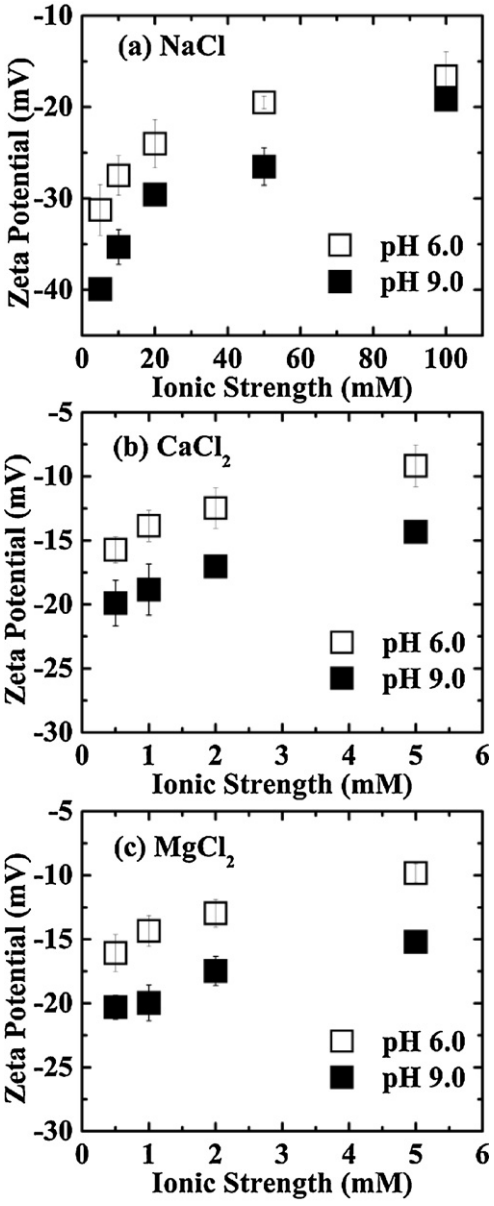

Fig. 1. Zeta potentials of MS2 in NaCl (a), $CaCl_2$ (b), and $MgCl_2$ solutions (c) at pH 6.0 (adjusted with 0.1 M HCl) and pH 9.0 (adjusted with 0.1 M NaOH) as a function of ionic strength. Each measurement was repeated 9–12 times. Error bars represent standard deviations.

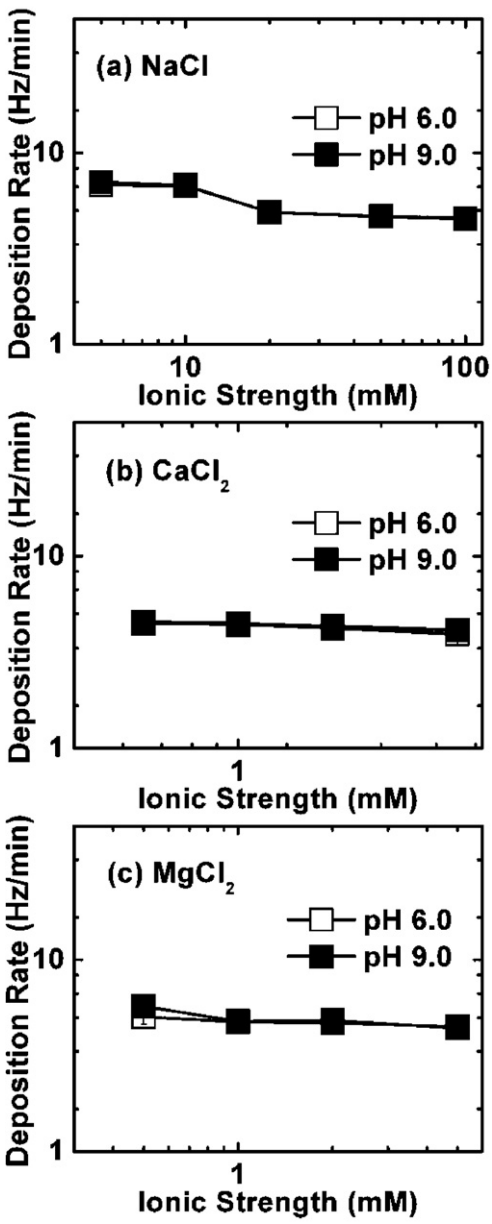

Fig. 2. Deposition rates of MS2 on PLL-coated surfaces in NaCl solutions (a), $CaCl_2$ solutions (b) and $MgCl_2$ solutions (c) at pH 6.0 (adjusted with 0.1 M HCl) and pH 9.0 (adjusted with 0.1 M NaOH) as a function of ionic strength. Duplicate measurements were conducted over entire ionic strength range ($n \geq 2$), with error bars representing standard deviations. The lines are meant to guide the eye.

(solid symbol) (Fig. 2a), which was in agreement with Yuan et al. [32]. The slight decrease of deposition rates with increasing ionic strength also held true in divalent $CaCl_2$ and $MgCl_2$ solutions (Fig. 2b and c). Moreover, at the same ionic strength (i.e. 5 mM), the deposition rates in monovalent NaCl solutions (6.8 Hz/min) were greater than those in divalent $CaCl_2$ (4.0 Hz/min) and $MgCl_2$ (4.2 Hz/min) solutions.

The greater particle deposition at low ionic strength relative to those at high ionic strength has been previously attributed to the formation of energy well at larger distance at low ionic strength [43–45]. To examine whether the slight decrease of deposition rates on PLL surfaces with increasing ionic strength observed in all examined salt solutions was also caused by the decreased separation distance of force well, DLVO interaction force profiles at representative conditions in both monovalent (NaCl) and divalent ($CaCl_2$ and $MgCl_2$) solutions were calculated and provided in Fig. 3. No repulsion force was present between MS2 and PLL-coated surface in all examined salt solutions, demonstrating favorable conditions for MS2 deposition on PLL-coated surfaces. In all examined salt (NaCl, $CaCl_2$, and $MgCl_2$) solutions, the force well formed at larger particle–surface distance at low ionic strength (e.g. 5 mM in NaCl) relative to those at high ionic strength (i.e. 50 mM in NaCl). Fig. 3 clearly showed that in both monovalent and divalent salt solutions, the separation distance at which MS2 started to experience attractive force decreased with increasing ionic strength, which was in consistent with the observed decrease of deposition rates with increasing ionic strength (Fig. 2). Moreover, at the same ionic strength, the force well located at larger distance in monovalent NaCl solutions relative to those in divalent $CaCl_2$ and $MgCl_2$ solutions, agreed with the greater deposition rate observed in NaCl solutions. The results showed that the slightly decreased deposition rates with increasing ionic strength observed for MS2 were

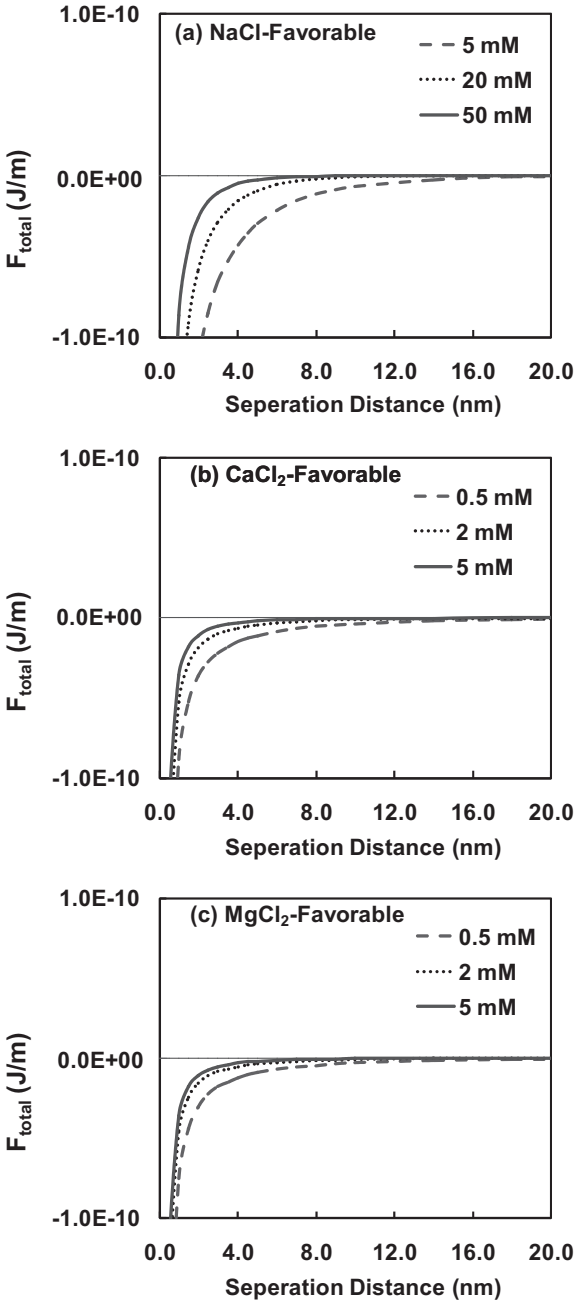

Fig. 3. Calculated DLVO interaction force between MS2 and PLL-coated surfaces at representative ionic strength in NaCl (a), $CaCl_2$ (b), and $MgCl_2$ (c) solutions at pH 6.0. The zeta potentials employed to calculate DLVO interaction force were provided in Figs. 1 and S1.

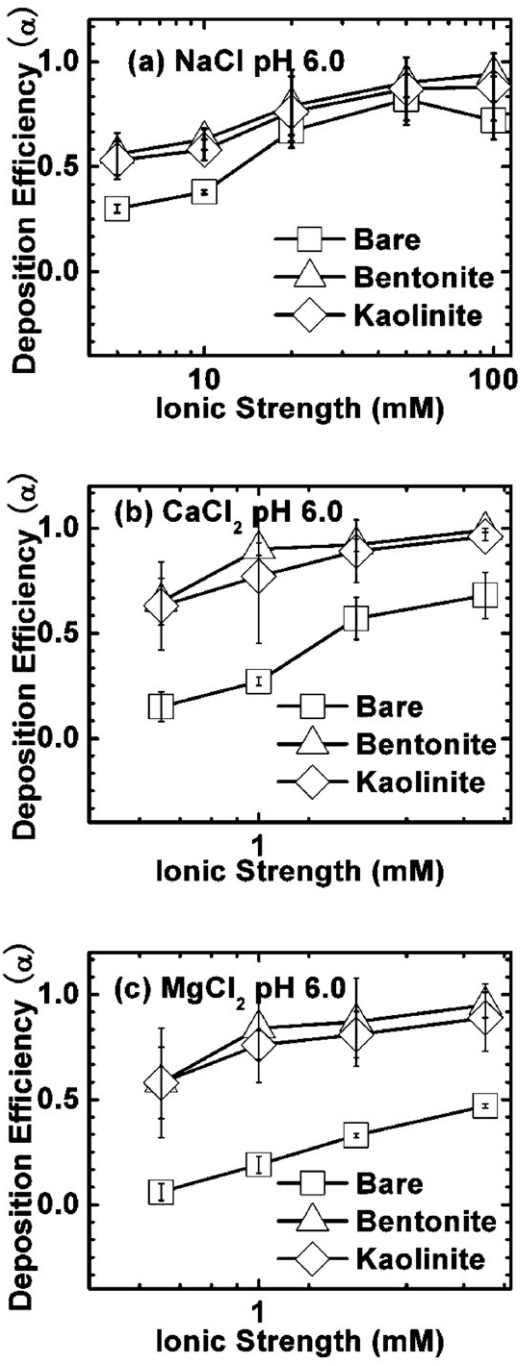

Fig. 4. Deposition efficiencies of MS2 on bare silica surfaces in NaCl solutions (a), $CaCl_2$ solutions (b), and $MgCl_2$ solutions(c) at pH 6.0 (adjusted with 0.1 M HCl) as a function of ionic strength. Duplicate measurements were conducted over entire ionic strength range ($n \geq 2$), with error bars representing standard deviations. The lines are meant to guide the eye.

also caused by the decrease of particle–surface separation distance of attractive force with increasing ionic strength.

3.3. MS2 deposition on bare silica surfaces

The deposition of MS2 on bare silica surfaces was examined in a wide range of solution ionic strengths in NaCl (5–100 mM), $CaCl_2$ (0.5–5 mM), and $MgCl_2$ (0.5–5 mM) solutions at pH 6.0 and pH 9.0. By normalizing the acquired deposition rates on bare silica surfaces by the favorable deposition rates on PLL-modified silica surfaces at corresponding electrolyte ionic strengths, the deposition efficiencies (α) of MS2 under all examined conditions were derived. In NaCl solutions, α of MS2 on bare silica increased with increasing ionic strength at both pH 6.0 (Fig. 4a, open square) and pH 9.0 (Fig. 5a, open square), agreed with Yuan et al. [32]. The same trends were also obtained in divalent $CaCl_2$ (Figs. 4b and 5b, open square) and $MgCl_2$ (Figs. 4c and 5c, open square) solutions at both pH conditions. The increased α with increasing solution ionic strength examined in all salt solutions at both pH conditions was consistent with the trends of zeta potentials versus ionic strength for both MS2 and silica (Figs. 1 and S1) and thus generally agreed with classic DLVO theory (Fig. 6). The increase of solution ionic strength led to the compression of electrostatic double layer

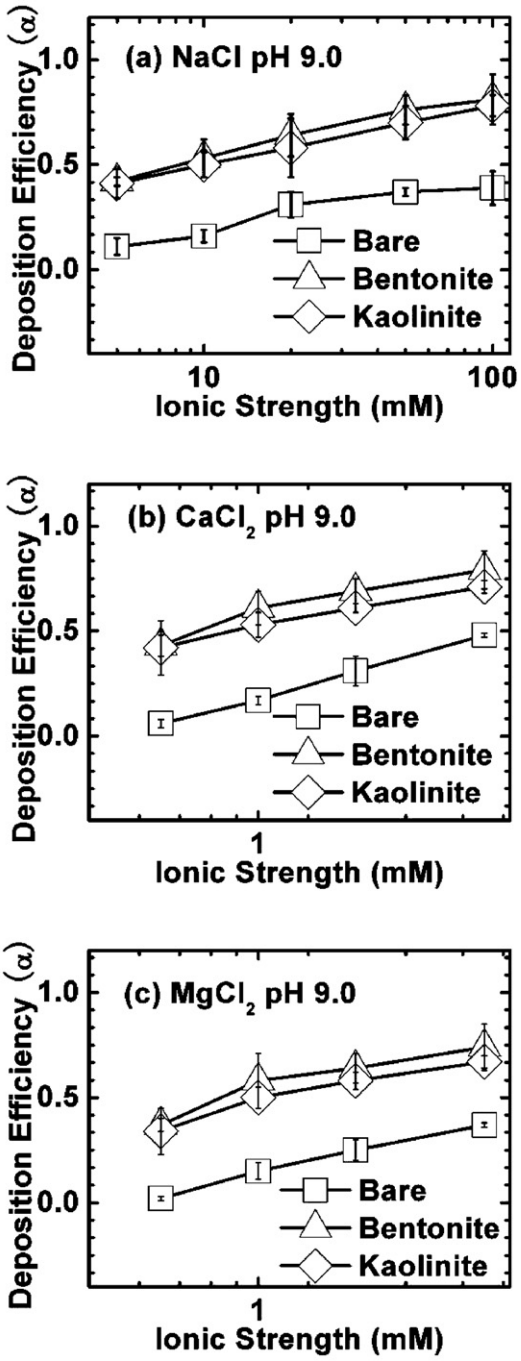

Fig. 5. Deposition efficiencies of MS2 on bare silica surfaces in NaCl solutions (a), $CaCl_2$ solutions (b), and $MgCl_2$ solutions(c) at pH 9.0 (adjusted with 0.1 M NaOH) as a function of ionic strength. Duplicate measurements were conducted over entire ionic strength range ($n \geq 2$), with error bars representing standard deviations. The lines are meant to guide the eye.

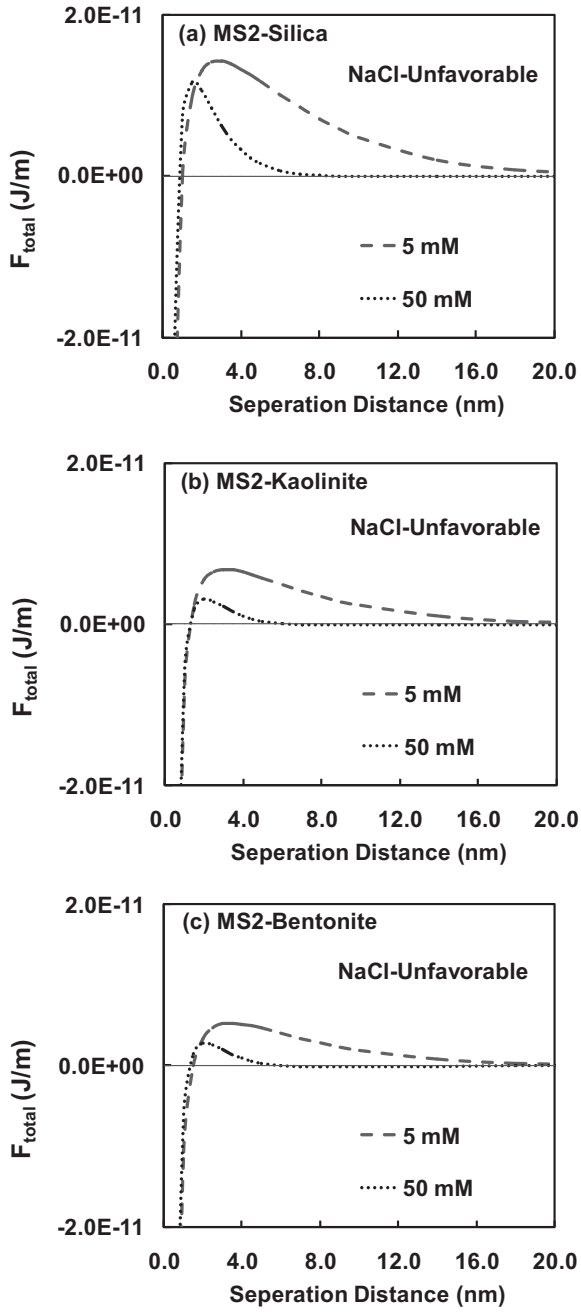

Fig. 6. Calculated DLVO interaction forces between MS2 and bare silica surface (a), MS2 and kaolinite-coated surface (b), MS2 and bentonite-coated surface (c) at representative ionic strength in NaCl solutions at pH 6.0. The zeta potentials employed to calculate DLVO interaction force were provided in Figs. 1 and S1.

between MS2 and silica surface, as a result, greater deposition efficiencies of MS2 were obtained at high ionic strength. At the same ionic strength (i.e. 5 mM), α obtained in divalent salt solutions (0.68 for $CaCl_2$ and 0.47 for $MgCl_2$ at pH 6.0) were greater than those in monovalent salt solutions (0.3 for NaCl). The greater colloid deposition in divalent salt solutions relative to that in monovalent solutions has been reported previously [46–48]. The observed greater α obtained in divalent salt solutions can be explained by DLVO theory. The complexation of divalent cations with functional groups on virus surfaces [49] resulted in the less negative zeta potentials of MS2 in divalent salt solutions (Fig. 1). Moreover, the binding of divalent ions to silanol groups of the silica surface [50] also reduced the charge of silica (Fig. S1). Therefore, in divalent salt solutions, the repulsive interaction between MS2 and silica was reduced comparing that in monovalent solutions. Comparison of α in $CaCl_2$ solutions versus those in $MgCl_2$ solutions yielded that at the same ionic strength, α obtained in $CaCl_2$ solutions (e.g. 0.68 at 5 mM and pH 6) were slightly greater than those in $MgCl_2$ solutions (e.g. 0.47 at 5 mM and pH 6) at both pH conditions. This held true for all examined ionic strength conditions. The greater deposition in Ca^{2+} salt solutions relative to those in Mg^{2+} salt solutions has also been previously observed for other microbes e.g. Rotavius

[20] and *Cryptosporidium parvum* oocysts [51]. This observation was also consistent with slightly less negative zeta potentials in $CaCl_2$ solutions than those in $MgCl_2$ solutions due to the greater binding ability of Ca^{2+} with functional groups on virus surfaces (Fig. 1). The above observations demonstrated that in all salt solutions containing monovalent or divalent cations, deposition of MS2 on bare silica surfaces was mainly controlled by DLVO interactions.

3.4. MS2 deposition on clay-coated silica surfaces

The significance of clay-coated silica surfaces on the deposition kinetics of MS2 was investigated in NaCl (5–100 mM), $CaCl_2$ (0.5–5 mM), and $MgCl_2$ (0.5–5 mM) solutions at pH 6.0 (Fig. 4) and pH 9.0 (Fig. 5). Similar to the observation on bare silica surface, α on clay-coated surface increased with increasing ionic strength in all salt solutions (monovalent or divalent cations) at both pH conditions. For example, in NaCl solutions at pH 6.0, α on bentonite-coated surfaces increased from 0.56 to 0.94 as ionic strength increased from 5 to 100 mM, similarly, α on kaolinite-coated silica surfaces increased from 0.53 to 0.88. The increase of α on both clay-coated surfaces with increasing ionic strength was consistent with less negative zeta potentials at high ionic strength for both MS2 and clay (Figs. 1 and S1) and thus agreed with DLVO theory (Fig. 6). Greater adsorption of virus to clay particles at high ionic strength has also been observed previously [8]. At same ionic strength (i.e. 5 mM), α of MS2 on both clay-coated surfaces obtained in divalent salt solutions (0.99 for $CaCl_2$ and 0.95 for $MgCl_2$ on bentonite-coated surfaces) were larger than that in monovalent NaCl solutions (0.56), which held true for both examined pH. Greater deposition on clay-coated surfaces in divalent salt solutions can be explained by the less negative zeta potentials of MS2 as well as clay-coated surfaces in divalent salt solutions (Figs. 1 and S1). The above observations clearly showed that, similar to deposition on bare silica surfaces, MS2 deposition on two examined clay (bentonite and kaolinite)-coated surfaces under all conditions regardless of ionic strength, ion types, and pH was also dominated by DLVO interactions.

3.5. Comparison of MS2 deposition on different surfaces

Comparison of α of MS2 on two clay-coated silica surfaces (Figs. 4 and 5, open diamond and open triangle) versus those on bare silica surfaces (Figs. 4 and 5, open square) showed that under all examined ionic strength conditions, deposition on two clay-coated surfaces was greater than those on bare silica surfaces in NaCl solutions at both pH 6.0 and pH 9.0. The same trends were also observed in divalent salt solutions ($CaCl_2$ and $MgCl_2$). For example, at 10 mM and pH 6.0 in NaCl solutions, α of MS2 on bare silica surfaces was 0.38, whereas α of MS2 on two clay-coated surfaces: bentonite and kaolinite coated surfaces were 0.63 and 0.58, respectively. These observations demonstrated that in all examined salt solutions regardless of ionic strength, ion types, and pH, clay (kaolinite and bentonite) deposited on silica surfaces significantly increased the deposition kinetics of MS2.

Greater deposition on clay coated-surfaces than that on bare silica surfaces was consistent with DLVO theory. Under all examined ionic strength conditions, zeta potentials of silica were more negative relative to those of two clay types (kaolinite and bentonite) both in monovalent (NaCl) and divalent salt ($CaCl_2$ and $MgCl_2$) solutions (Fig. S1). The interaction force between MS2 and clay coated-surfaces therefore was less repulsive relative to that between MS2 and silica under all examined conditions (Fig. 6), resulting in the greater deposition on clay-coated surfaces. The adsorption of virus to clay has been previously attributed to the non-DLVO interaction forces such as hydrogen bonding and the formation of a cation bridge between virus and clay [52,53]. The anionic groups of the clay and MS2 might also form hydrogen bonds, resulting in the enhanced deposition on clay-coated surfaces. Correlation of virus adsorption to clay with CEC or AEC of clay (bentonite and kaolinite) has also been demonstrated previously, thus the cation or anion exchange reactions of clay has been proposed as an important mechanism contributing to the adsorption of virus to clay [8,54–56]. Cation and anion exchange sites are present on bentiontie and kaolinite, two clays examined in this study. Therefore, the cation or anion exchange reactions of bentiontie/kaolinite would be expected, which resulted in the greater deposition observed on clay-coated surfaces relative to on bare silica.

Previous studies e.g. Schiffenbauer and Stotzky [55] pointed out that the adsorption of Coliphage T1 has direct correlation with the ratio AEC/CEC ratio of clays. Although kaolinite has a larger AEC/CEC ratio than bentonite [57], the deposition of MS2 on kaolinite-coated surfaces (open diamond) were slightly less relative to those on bentonite-coated surfaces (open triangle). For example α on bentonite-coated surfaces at 1 mM and pH 6 in $MgCl_2$ solutions were 0.84, whereas α on kaolinite-coated surfaces under the same conditions were 0.76. The observation demonstrated that the deposition of MS2 on clay-coated surfaces did not correlate with AEC/CEC ratio of clays. The less deposition on kaolinite-coated surfaces than on bentonite-coated surfaces might be due to the slightly more negative zeta potentials of kaolinite-coated surfaces relative to those of bentonite-coated surfaces (Fig. S1). The more negative zeta potentials of kaolinite relative to those of bentonite have also been reported in Syngouna and Chrysikopoulos [34].

4. Conclusion

To the best of our knowledge, this study for the first time compared the deposition behavior of MS2 on bare silica, PLL-coated silica surfaces, and clay (kaolinite and bentonite) coated surfaces over a wide range of environmentally relevant ionic strength in both monovalent (NaCl) and divalent ($CaCl_2$ and $MgCl_2$) solutions at both pH 6.0 and pH 9.0. Our study found that in all examined salt solutions regardless of ion types, the deposition rate of MS2 on PLL-coated silica decreased with increasing ionic strength due to the decreased separation distance of attractive force well. Deposition kinetics of MS2 increased with increasing solutions ionic strength both on bare and clay-coated silica surfaces, which agreed with DLVO theory. Deposition kinetics on both bare and clay-coated surfaces dramatically increased with the presence of divalent ions (Ca^{2+} and Mg^{2+}) in solutions. Coating silica surfaces with clay (either kaolinite or bentonite) significantly increased MS2 deposition.

Supplementary information

Zeta potentials of crushed quartz sand, clay-coated crushed sand, and PLL-coated quartz sand particle (Fig. S1); also presented are details about protocol for MS2 deposition experiments on PLL coated silica surfaces, protocol of adsorbing clay on silica surface, influence of solution chemistry on zeta potentials of different surfaces, and calculation of Hamaker constant for MS2–water–PLL system.

Acknowledgments

This work was supported by the National Natural Science Foundation of China under grants no. 21177002 and no. 40802054. This research was also in part supported by the National Research Foundation of Korea Grant funded by the Korean Government (MEST) (NRF-2010-0023782). The authors wish to acknowledge

Prof. Thanh H. Nguyen from Department of Civil and Environmental Engineering at University of Illinois at Urbana-Champaign, the editor, and two reviewers for their very helpful comments. We are also grateful to Professor Alistair Borthwick from the University of Oxford for his kind help in English editing.

Appendix A. Supplementary data

Supplementary data associated with this article can be found, in the online version, at doi:10.1016/j.colsurfb.2011.12.017.

References

[1] R. Anders, C.V. Chrysikopoulos, Water Resour. Res. 41 (2005).
[2] S.A. Bradford, Y.F. Tadassa, Y. Jin, J. Environ. Qual. 35 (2006) 1692–1701.
[3] K.R. Calci, W. Burkhardt, W.D. Watkins, S.R. Rippey, Appl. Environ. Microb. 64 (1998) 5027–5029.
[4] C. Masciopinto, R. La Mantia, C.V. Chrysikopoulos, Water Resour. Res. 44 (2008).
[5] M.V. Yates, Ground Water 23 (1985) 586–591.
[6] C.P. Gerba, C. Wallis, J.L. Melnick, Environ. Sci. Technol. 9 (1975) 1122–1126.
[7] J.L. Melnick, C.P. Gerba, C. Wallis, Bull. World Health Organ. 56 (1978) 499–508.
[8] S.M. Lipson, G. Stotzky, Appl. Environ. Microb. 46 (1983) 673–682.
[9] G.F. Craun, N. Nwachuku, R.L. Calderon, M.F. Craun, J. Environ. Health 65 (2002) 16–23.
[10] G.F. Craun, Water Sci. Technol. 24 (1991) 17–20.
[11] M.H. Kramer, B.L. Herwaldt, G.F. Craun, R.L. Calderon, D.D. Juranek, J. Am. Water Works Assoc. 88 (1996) 66–80.
[12] M.V. Yates, S.R. Yates, J. Wagner, C.P. Gerba, J. Contam. Hydrol. 1 (1987) 329–345.
[13] R.C. Bales, S.R. Hinkle, T.W. Kroeger, K. Stocking, C.P. Gerba, Environ. Sci. Technol. 25 (1991) 2088–2095.
[14] Y. Jin, Y.J. Chu, Y.S. Li, J. Environ. Qual. 43 (2000) 111–128.
[15] Y. Chu, Y. Jin, M.V. Yates, J. Environ. Qual. 29 (2000) 1103–1110.
[16] J. Han, Y. Jin, C.S. Willson, Environ. Sci. Technol. 40 (2006) 1547–1555.
[17] P.S.K. Knappett, M.B. Emelko, J. Zhuang, L.D. Mckay, Water Res. 42 (2008) 4368–4378.
[18] G. Sadeghi, J.F. Schijven, T. Behrends, S.M. Hassanizadeh, J. Gerritse, P.J. Kleingeld, Ground Water 49 (2011) 12–19.
[19] J. Zhuang, Y. Jin, J. Contam. Hydrol. 60 (2003) 193–209.
[20] L. Gutierrez, S.E. Mylon, B. Nash, T.H. Nguyen, Environ. Sci. Technol. 44 (2010) 4552–4557.
[21] R.C. Bales, S.M. Li, K.M. Maguire, M.T. Yahya, C.P. Gerba, Water Resour. Res. 29 (1993) 957–963.
[22] J.N. Ryan, M. Elimelech, R.A. Ard, R.W. Harvey, P.R. Johnson, Environ. Sci. Technol. 33 (1999) 63–73.
[23] G.E. Walshe, L.P. Pang, M. Flury, M.E. Close, M. Flintoft, Water Res. 44 (2010) 1255–1269.
[24] S. Van Cuyk, R.L. Siegrist, Water Res. 41 (2007) 699–709.
[25] M.D. Sobsey, C.H. Dean, M.E. Knuckles, R.A. Wagner, Appl. Environ. Microb. 40 (1980) 92–101.
[26] J. Zhuang, Y. Jin, J. Environ. Qual. 32 (2003) 816–823.
[27] A.P. Pieper, J.N. Ryan, R.W. Harvey, G.L. Amy, T.H. Illangasekare, D.W. Metge, Environ. Sci. Technol. 31 (1997) 1163–1170.
[28] J.W.A. Foppen, S. Okletey, J.F. Schijven, J. Contam. Hydrol. 85 (2006) 287–301.
[29] Y. Jin, E. Pratt, M.V. Yates, J. Environ. Qual. 29 (2000) 532–539.
[30] R.A. Abudalo, Y.G. Bogatsu, J.N. Ryan, R.W. Harvey, D.W. Metge, M. Elimelech, Environ. Sci. Technol. 39 (2005) 6412–6419.
[31] Y.J. Chu, Y. Jin, T. Baumann, M.V. Yates, J. Environ. Qual. 32 (2003) 2017–2025.
[32] B.L. Yuan, M. Pham, T.H. Nguyen, Environ. Sci. Technol. 42 (2008) 7628–7633.
[33] R. Attinti, J. Wei, K. Kniel, J.T. Sims, Y. Jin, Environ. Sci. Technol. 44 (2010) 2426–2432.
[34] V.I. Syngouna, C.V. Chrysikopoulos, Environ. Sci. Technol. 44 (2010) 4539–4544.
[35] F.J. Galindo-Rosales, F.J. Rubio-Hernandez, Appl. Clay Sci. 33 (2006) 109–115.
[36] L.W. Mays, Water Resources Handbook, 1996.
[37] A.J. de Kerchove, M. Elimelech, Macromolecules 39 (2006) 6558–6564.
[38] A.J. de Kerchove, P. Weronski, M. Elimelech, Langmuir 23 (2007) 12301–12308.
[39] R. Hogg, T.W. Healy, D.W. Ferstenau, Trans. Faraday Soc. 62 (1966) 1638–1651.
[40] S.L. Penrod, T.M. Olson, S.B. Grant, Langmuir 12 (1996) 5576–5587.
[41] T. Kohn, M. Grandbois, K. McNeill, K.L. Nelson, Environ. Sci. Technol. 41 (2007) 4626–4632.
[42] Q.L. Li, M. Elimelech, Environ. Sci. Technol. 38 (2004) 4683–4693.
[43] M. Elimelech, J. Colloid Interface Sci. 146 (1991) 337–352.
[44] M. Elimelech, L. Song, Sep. Sci. Technol. 2 (1992) 2–12.
[45] J. Fatisson, R.F. Domingos, K.J. Wilkinson, N. Tufenkji, Langmuir 25 (2009) 6062–6069.
[46] K.L. Chen, M. Elimelech, Environ. Sci. Technol. 42 (2008) 7607–7614.
[47] T.H. Nguyen, M. Elimelech, Biomacromolecules 8 (2007) 24–32.
[48] P.T. Zhu, G.Y. Long, J.R. Ni, M.P. Tong, Environ. Sci. Technol. 43 (2009) 5699–5704.
[49] S.E. Mylon, C.I. Rinciog, N. Schmidt, L. Gutierrez, G.C.L. Wong, T.H. Nguyen, Langmuir 26 (2010) 1035–1042.
[50] J.A. Libera, H. Cheng, M.O. de la Cruz, M.J. Bedzyk, J. Phys. Chem. B 109 (2005) 23001–23007.
[51] D. Janjaroen, Y.Y. Liu, M.S. Kuhlenschmidt, T.B. Kuhlenschmidt, T.H. Nguyen, Environ. Sci. Technol. 44 (2010) 4519–4524.
[52] G. Stotzky, Microbial Adhesion to Surfaces, Ellis Harwood Ltd., Chichester, 1980.
[53] G.F. Carlson, F.E. Woodard, D.F. Wentworth, O.J. Sproul, J. Water Pollut. Control. Fed. 40 (1968) R89.
[54] M. Schiffenbauer, G. Stotzky, Curr. Microbiol. 8 (1983) 245–249.
[55] M. Schiffenbauer, G. Stotzky, Appl. Environ. Microb. 43 (1982) 590–596.
[56] S.W. Funderburg, B.E. Moore, B.P. Sagik, C.A. Sorber, Water Res. 15 (1981) 703–711.
[57] R.E. Grim, Clay Mineralogy, McGraw-Hill Book Co., New York, 1968.